J. Fluid Mech. (1989), *vol.* 204, *pp.* 405–420
Printed in Great Britain

On the onset of three-dimensionality and time-dependence in Görtler vortices

By PHILIP HALL[1] AND SHARON SEDDOUGUI[2]

[1] Mathematics Department, Exeter University, North Park Road, Exeter EX4 4QE, UK

[2] Institute for Computer Applications in Science and Engineering, NASA Langley Research Center, Hampton, VA 23665, USA

(Received 14 December 1987 and in revised form 24 January 1989)

The secondary instability of large-amplitude Görtler vortices in a growing boundary layer is discussed in the fully nonlinear regime. It is shown that the three-dimensional breakdown to a flow with wavy vortex boundaries, similar to that which occurs in the Taylor vortex problem takes place. However, the instability is confined to the thin shear layers which were shown by Hall & Lakin (1988) to trap the region of vortex activity. The disturbance eigenfunctions decay exponentially away from the centre of these layers, so that the upper and lower shear layers can support independent modes of instability. The structure of the instability, in particular its location and speed of downstream propagation, is found to be entirely consistent with recent experimental results. Furthermore, it is shown that the upper and lower layers support wavy vortex instabilities with quite different frequencies. This result is again consistent with the available experimental observations.

1. Introduction

Our concern is with the nature of the three-dimensional breakdown of steady, spanwise periodic large-amplitude Görtler vortices. It is known from the experiments of Bippes & Görtler (1972) and Aihara & Koyama (1981) that this breakdown leads to a time-periodic flow with wavy vortex boundaries similar to those which occur in the Taylor problem. More recently Kohama (1987) has investigated vortex instabilities in boundary-layer flows over a laminar flow wing. He found a secondary instability of Görtler vortices localized at the top of the region of vortex activity. Furthermore, Kohama found that the instability propagated downstream with a speed that approached the free-stream speed as it developed in the downstream direction. The onset of this time-dependent motion was found in all of the above experiments to be ultimately followed by transition to turbulence. At this stage more obvious differences between the Görtler and Taylor problems emerge so that, for example, the rich bifurcation structure of the Taylor problem is apparently not carried over to the Görtler problem.

In fact even in the linear regime the apparent similarities between Taylor and Görtler vortices are perhaps misleading, since it is known from the work of Hall (1982*a*, *b*, 1983, 1984) that non-parallel effects in the Görtler problem cannot in general be ignored. Indeed it was shown by Hall (1983) that the inconsistencies of the various parallel-flow theories of for example Görtler (1940), Hämmerlin (1956) and later authors are a direct consequence of the parallel-flow approximation. The only regime where this difficulty with the parallel-flow theories does not occur is at small vortex wavelengths where the effect of boundary-layer growth on the vortices

becomes less important. However, the most surprising feature of the non-parallel theory of Hall (1983) is that the concept of a unique neutral wave is not tenable in the Görtler problem. This is because the downstream position where a vortex begins to grow is a function of the location and initial form of the imposed disturbance. A more significant consequence of the non-parallel theory is that the concept of a unique growth rate at a given downstream location is also not tenable. This result makes transition prediction by empirical methods such as the e^n rule not possible. Nevertheless, there is much work still being done in the context of 'parallel-flow' Görtler vortices.

The non-uniqueness properties of solutions of the correct zeroth-order approximations to the linear Görtler vortex equations were shown by Hall (1988) to occur in the corresponding nonlinear problem at $O(1)$ wavenumbers. In the latter paper, the development of finite-amplitude Görtler vortices was investigated numerically using a finite-difference discretization in the normal and chordwise directions together with a Fourier expansion in the spanwise direction. It was found that as the vortices move downstream the disturbance energy flow becomes concentrated in the fundamental and the mean flow correction. This is entirely consistent with the weakly nonlinear theory of Hall (1982*b*) which is appropriate to small-wavelength vortices. However, in a growing boundary layer, the 'local' wavenumber of a fixed-wavelength disturbance grows like the displacement thickness of the boundary layer. Thus, in most flows any vortex will eventually enter the small-wavelength regime where locally the asymptotic analysis of Hall (1982*a*, *b*) apply.

As is the case with all weakly nonlinear stability calculations, the work of Hall (1982*b*) is restricted to a neighbourhood of the position where a given disturbance is neutrally stable. However, with the boundary-layer thickness as an appropriate lengthscale, it can be inferred from the calculation that a vortex of non-dimensional wavenumber ϵ^{-1}, where $0 < \epsilon \ll 1$, reinforces the basic flow at zeroth order at a distance $O(\epsilon)$ downstream of the neutral point. This result was recently developed by Hall & Lakin (1988, hereinafter referred to as HL), to give an asymptotic description of fully nonlinear Görtler vortices at distances beyond the neutral point comparable with the distance from the leading edge. It is the instability of this type of vortex that we will investigate in this paper. However, before discussing the nature of this instability we need to point out the salient properties of the HL calculations.

Consider then a Görtler vortex of wavenumber ϵ^{-1} developing in a boundary-layer flow with Görtler number of $O(\epsilon^{-4})$. This choice of small-wavelength vortices is not as restrictive as it might first appear since, as explained above, this regime is always approached by a fixed-wavelength vortex in a growing boundary layer. Suppose further that the flow is neutrally stable at the downstream location $x = x_n$, then HL showed that for $x > x_n$ the flow field splits up as shown in figure 1. The vortex activity is confined to region I and decays exponentially to zero in the thin shear layers II*a*, *b*. In regions III*a*, *b* there is no vortex activity and the mean flow satisfies the boundary-layer equations. However, in region I the mean flow is determined as a solvability condition on equations for the fundamental. In fact, the mean flow adjusts itself so as to make the fundamental and all the higher harmonics finite in I. The mean flow equations then determine the vortex velocity field in I. Thus, there is a complete reversal of the usual roles of the mean flow and harmonic equations compared to say the situation in flows where nonlinearity can be described by the Stuart–Watson method. The shear layers located at y_1 and y_2 change position as they move downstream; their positions are determined from the solution of a double free-

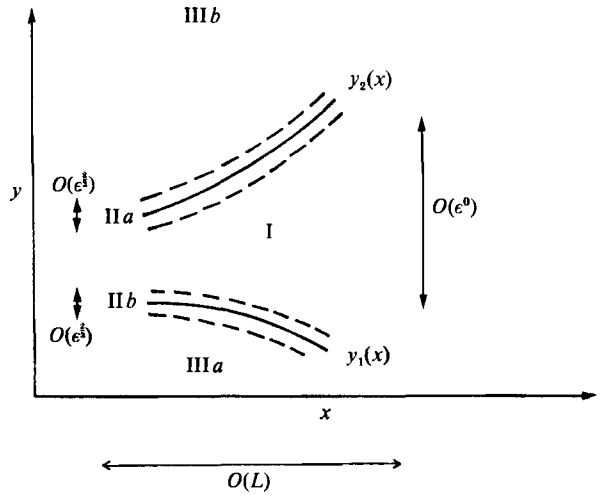

FIGURE 1. The different regions beyond the downstream position of neutral stability.

boundary problem associated with the boundary layer-equations. However, in flows where the local Görtler number increases faster than the fourth power of the local wavenumber HL showed that y_1 migrates to the wall whilst y_2 moves to or beyond the edge of the boundary layer. The mean downstream velocity components in the layers IIa, b then approach the free-stream speed and zero respectively. This has fundamental implications for the time-dependent structure of the breakdown of this flow.

We shall seek secondary instabilities of the flow in layers IIa, b; more precisely we superimpose spanwise periodic travelling waves on the flow in these layer and see how they develop. These perturbations are $\frac{1}{2}\pi$ radians out of phase with the fundamental in the spanwise direction, so that if the secondary instability occurs it will produce locally wavy vortex boundaries in IIa, b. It is of course not obvious that, should wavy vortices occur, the regions IIa, b should be particularly susceptible to these modes. In order to see why this is the case, we consider the model equation

$$\left\{\frac{\partial^2}{\partial y^2}-y\frac{\partial}{\partial x}-\frac{\partial}{\partial t}-\tfrac{1}{4}y^2+\lambda\right\}\psi=\psi|\psi|^2, \tag{1.1}$$

together with the condition $\psi\to 0, |y|\to\infty$.

In fact, this equation essentially governs the nonlinear growth of time-dependent Görtler vortices in curved channel flows. Here λ is a parameter, t denotes time, x is the distance around the channel, and y is the distance from the centre of the internal viscous layer where the vortices initially develop. A finite-amplitude solution of (1.1) representing a steady, x-independent vortex $\psi=\psi_{\mathrm{v}}$ satisfies

$$\left\{\frac{\partial^2}{\partial y^2}-\tfrac{1}{4}y^2+\lambda\right\}\psi_{\mathrm{v}}=\psi_{\mathrm{v}}^3. \tag{1.2}$$

The instability of this flow to a travelling vortex-like perturbation can be calculated by setting

$$\psi=\psi_{\mathrm{v}}+\psi'(x,y,t),$$

where ψ' is a real function of x, y and t. If we now look at disturbances with $\psi' = \mathrm{Re}\,(\mathrm{e}^{\mathrm{i}kx+\sigma t}\phi(y))$ then we find that $\phi(y)$ satisfies

$$\left(\frac{\partial^2}{\partial y^2} - \tfrac{1}{4}y^2 + \lambda - \mathrm{i}ky - \sigma\right)\phi = 3\psi_{\mathrm{v}}^2\phi, \quad \phi \to 0, |y| \to \infty, \tag{1.3}$$

which determines an eigenrelation $\sigma = \sigma(k)$. However if the wave is $\frac{1}{2}\pi$ radians out of phase in the spanwise direction with the fundamental vortex then (1.3) becomes

$$\left(\frac{\partial^2}{\partial y^2} - \tfrac{1}{4}y^2 + \lambda - \mathrm{i}ky - \sigma\right)\phi = \psi_{\mathrm{v}}^2\phi, \quad \phi \to 0, |y| \to \infty. \tag{1.4}$$

The latter eigenvalue problem was studied by Shaw (1983) who found that unstable modes occur for $\lambda = O(1)$. (In contrast to this result (1.3) leads to stable disturbances.) Here λ plays the role of Görtler number so that increasing λ is equivalent to increasing x for the boundary-layer problem. Of more relevance to our problem is the solution of (1.4) for $\lambda \gg 1$. In this case ψ_{v} develops a triple-layer structure with a core region with $\psi_{\mathrm{v}} = (\lambda - \frac{1}{4}y^2)^{\frac{1}{2}}$ trapped between shear layers of thickness $\lambda^{-\frac{1}{6}}$ at $y = \pm(4\lambda)^{\frac{1}{2}}$. These shear layers correspond to $\mathrm{II}a, b$ in the HL calculation. An examination of (1.4) in this limit shows that any eigenvalues must now concentrate in $\mathrm{II}a, b$ because in the core ϕ now satisfies

$$\left(\frac{\partial^2}{\partial y^2} - \mathrm{i}ky - \sigma\right)\phi = 0.$$

This is an Airy equation so that $\phi \to \infty$ when $y \to \infty$ or $y \to -\infty$, in which case ϕ is exponentially large as one of the shear layers is approached. Hence, matching with the corresponding solution in the shear layers cannot be achieved. Thus, any disturbances in the model problem must concentrate in the shear layers and decay away from the centres of the layers. We do not solve the model problem in the shear layers but merely use the above argument to suggest that any disturbances for the boundary-layer problem will, if they exist, concentrate in the shear layers. The disturbances will be made to decay exponentially away from the shear layers so that, unless exponentially small terms are matched, the layers can be treated independently. Furthermore, the number of modes associated with an instability in either shear layer is not fixed by a discussion of the model problem.

The above structure for the model equation is sufficiently close to the boundary-layer problem for it to be applicable there. Thus, after formulating our instability equations in §2 we shall in §3 investigate the instability of $\mathrm{II}a, b$ to wavy vortex modes. In §4 we present the results of our calculation and draw some conclusions.

2. Formulation of the problem

The flow under consideration is that described by HL. We consider the flow of an incompressible, viscous fluid of kinematic viscosity ν and density $\bar{\rho}$, over a wall of variable concave curvature $\rho\chi(X/L)$. Here ρ^{-1} is a typical radius of curvature, X denotes distance along the wall and L is a typical lengthscale along the wall. The Reynolds number for the flow, R_E, is defined by

$$R_E = \frac{U_0 L}{\nu}, \tag{2.1}$$

where U_0 is a typical flow velocity. A curvature parameter, δ_c, is defined by

$$\delta_c = \rho L. \tag{2.2}$$

We are interested in the limit $R_E \to \infty$ with the Görtler number G, defined by

$$G = 2R_E^{\frac{1}{2}}\delta_c, \tag{2.3}$$

held fixed. We denote time by T and (X, Y, Z) are taken to be the coordinates along the wall, normal to the wall and in the spanwise direction respectively. If (U, V, W) denotes the corresponding velocity vector we define dimensionless coordinates (x, y, z) and velocity (u, v, w) by

$$(x, y, z) = L^{-1}(X, YR_E^{\frac{1}{2}}, ZR_E^{\frac{1}{2}}),$$

and

$$(u, v, w) = U_0^{-1}(U, VR_E^{\frac{1}{2}}, WR_E^{\frac{1}{2}}).$$

Our analysis is restricted to flows with $u \to 1$ when $y \to \infty$ and the pressure P is written in the form

$$P = \bar{\rho}\frac{U_0^2}{R_E}p.$$

The continuity equation and non-dimensional unsteady Navier–Stokes equations for the flow take the form

$$\frac{\partial u}{\partial x} + \frac{\partial v}{\partial y} + \frac{\partial w}{\partial z} = 0, \tag{2.4a}$$

$$\frac{\partial u}{\partial t} + u\frac{\partial u}{\mathrm{d}x} + v\frac{\partial u}{\partial y} + w\frac{\partial u}{\partial z} = \frac{\partial^2 u}{\partial y^2} + \frac{\partial^2 u}{\partial z^2}, \tag{2.4b}$$

$$\frac{\partial v}{\partial t} + u\frac{\partial v}{\partial x} + v\frac{\partial v}{\partial y} + w\frac{\partial v}{\partial z} = -\tfrac{1}{2}G\chi u^2 - \frac{\partial p}{\partial y} + \frac{\partial^2 v}{\partial y^2} + \frac{\partial^2 v}{\partial z^2}, \tag{2.4c}$$

$$\frac{\partial w}{\partial t} + u\frac{\partial w}{\partial x} + v\frac{\partial w}{\partial y} + w\frac{\partial w}{\partial z} = -\frac{\partial p}{\partial z} + \frac{\partial^2 w}{\partial y^2} + \frac{\partial^2 w}{\partial z^2}. \tag{2.4d}$$

Here the non-dimensional time variable t is given by $t = U_0 L^{-1} T$, and terms of order $R_E^{-\frac{1}{2}}$ have been neglected. HL obtained a steady solution of (2.4) which satisfies

$$u = v = w = 0, \quad y = 0, \tag{2.5a, b}$$

$$\mathrm{u} \to 1, \quad y \to \infty.$$

This was an asymptotic solution valid in the limit of small vortex wavelength. The Görtler number G, defined in (2.3), is expanded in the form

$$G = G_0\epsilon^{-4} + G_1\epsilon^{-3} + \ldots, \tag{2.6}$$

where ϵ^{-1} is the non-dimensional wavenumber of the vortices. In the main part of the boundary layer $\bar{u}(x, y)$, the zeroth-order, z-independent part of the downstream velocity component satisfies

$$G_0\chi\bar{u}\frac{\partial\bar{u}}{\partial y} = 1.$$

This reflects the fact that here the mean flow is driven by finite-amplitude vortices. Here the effect of the vortices is to produce a mean flow correction the same size as the basic flow. Thus, the mean flow bears no resemblance to the flow that occurs when no vortices are present. The velocity field of the (smaller) vortices is then found by considering the z-independent part of the equations of motion in I. This calculation shows that the vortices are trapped between y_1 and y_2 and formally decay

to zero exponentially in IIa, b.It is found that the region I of vortex activity grows as the flow develops, eventually occupying the extent of the original boundary layer. Above y_2 and below y_1 there is no z-dependence to the flow and it is obtained by solving the boundary-layer equations with jump conditions at y_1, y_2. The shear layers IIa, b correspond to the $\lambda^{-\frac{1}{6}}$ layers for the model problem and we now examine the flow structure in IIa. In fact our analysis is equally applicable to region IIb so our theory determines the stability of both shear layers which trap the vortices. In order to investigate the instability of the boundary layer in this region we consider perturbations to the steady, basic flow satisfying (2.4) and (2.5) in region IIa.

3. The asymptotic structure of the wavy modes

It was shown by HL that layers IIa, b are of thickness $\epsilon^{\frac{2}{3}}$ so that in IIa we write

$$\xi = \frac{(y-y_2)}{\epsilon^{\frac{2}{3}}},$$

where $y_2(x)$ is the location of the layer IIa. The vortex activity of the steady flow is confined to the region I between the shear layers II$a,b$. The algebraically decaying vortices in region I are reduced to zero exponentially in the shear layers. Above y_2 and below y_1 the basic flow satisfies the boundary-layer equations. Thus, in IIa we replace $\partial/\partial x$ by

$$\frac{\partial}{\partial x} - \frac{y_2'}{\epsilon^{\frac{2}{3}}}\frac{\partial}{\partial \xi}$$

and $\partial/\partial y$ by

$$\frac{1}{\epsilon^{\frac{2}{3}}}\frac{\partial}{\partial \xi}.$$

The basic, steady expansions in IIa, satisfying (2.4) and (2.5), are given by equation (3.10) in HL and can be written in the form

$$u = u_{\mathrm{B}} = \bar{u}_0 + \epsilon^{\frac{2}{3}}\bar{u}_1 + \ldots + \epsilon^{\frac{4}{3}}\cos\left(\frac{z}{\epsilon}\right)(U_{01} + \epsilon^{\frac{2}{3}}U_{11} + \ldots) + \epsilon^2\cos\left(\frac{2z}{\epsilon}\right)(U_{02} + \epsilon^{\frac{2}{3}}U_{12} + \ldots) + \ldots, \quad (3.1a)$$

$$v = v_{\mathrm{B}} = \bar{v}_0 + \epsilon^{\frac{2}{3}}\bar{v}_1 + \ldots + \epsilon^{-\frac{2}{3}}\cos\left(\frac{z}{\epsilon}\right)(V_{01} + \epsilon^{\frac{2}{3}}V_{11} + \ldots) + \epsilon^2\cos\left(\frac{2z}{\epsilon}\right)(V_{02} + \epsilon^{\frac{2}{3}}V_{12} + \ldots) + \ldots, \quad (3.1b)$$

$$w = w_{\mathrm{B}} = \epsilon^{-\frac{1}{3}}\sin\left(\frac{z}{\epsilon}\right)(W_{01} + \epsilon^{\frac{2}{3}}W_{11} + \ldots) + \epsilon^{\frac{1}{3}}\sin\left(\frac{2z}{\epsilon}\right)(W_{02} + \epsilon^{\frac{2}{3}}W_{12} + \ldots) + \ldots, \quad (3.1c)$$

$$p = p_{\mathrm{B}} = \bar{p}_0 + \epsilon^{\frac{2}{3}}\bar{p}_1 + \ldots + \epsilon^{-\frac{4}{3}}\cos\left(\frac{z}{\epsilon}\right)(P_{01} + \epsilon^{\frac{2}{3}}P_{11} + \ldots) + \epsilon^{-\frac{2}{3}}\cos\left(\frac{2z}{\epsilon}\right)(P_{02} + \epsilon^{\frac{2}{3}}P_{12} + \ldots) + \ldots, \quad (3.1d)$$

where the coefficients are functions of x and ξ. In fact $\bar{u}_0$ is just the value of the mean streamwise velocity component in the shear layer and so is independent of ξ. Note that the coefficients $U_{jk}, V_{jk}, W_{jk}, P_{jk}$ in the above formulation correspond to $2U_{jk}, 2V_{jk}$, $2\mathrm{i}W_{jk}, 2P_{jk}$ respectively, $j = 0, 1, 2, \ldots, k = 1, 2, 3\ldots$, in the formulation of HL. The

equations obtained from substitution of the basic expansions (3.1) into the continuity and Navier–Stokes equations (2.4) and equating coefficients of like powers of ϵ are given in detail by HL. It is useful here to note that from (3.12) of HL

$$\bar{u}_0 = \frac{(a+2y_2)^{\frac{1}{2}}}{(G_0\chi)^{\frac{1}{2}}}, \tag{3.2a}$$

$$u_1 = \frac{\xi}{(G_0\chi)^{\frac{1}{2}}(a+2y_2)^{\frac{1}{2}}}. \tag{3.2b}$$

The equation which determines V_{01}, obtained from (3.1*b*), is

$$\frac{\partial^2 V_{01}}{\partial\xi^2} + g_1\xi V_{01} = \tfrac{1}{6}V_{01}^3 - g_2 f V_{01}, \tag{3.3}$$

where

$$g_1(x) = \frac{1}{3}\left(\frac{1}{a+2y_2} - \frac{\chi'(a+2y_2)^{\frac{3}{2}}}{3\chi(G_0\chi)^{\frac{1}{2}}} - b\right), \tag{3.4a}$$

and

$$g_2(x) = \tfrac{1}{3}(G_0\chi)^{\frac{1}{2}}(a+2y_2)^{\frac{1}{2}}. \tag{3.4b}$$

Here $f(x)$ is a function that can only be determined at higher order, $a(x)$ and $b(x)$ are arbitrary functions of x arising from the solution in region I (see (3.7) in HL), and a prime denotes a derivative with respect to x.

Since the solution of (3.3) is required in the later analysis, we shall give a description of it here. In order to eliminate $f(x)$ from (3.3) we introduce the variable ξ_1 and let

$$\xi = \xi_1 - \frac{g_2 f}{g_1}, \tag{3.5}$$

so that (3.3) becomes

$$\frac{\partial^2 V_{01}}{\partial\xi_1^2} + g_1\xi_1 V_{01} = \tfrac{1}{6}V_{01}^3. \tag{3.6}$$

In order to simplify (3.6) further we make the transformations

$$\eta = (-g_1)^{\frac{1}{3}}\xi_1, \tag{3.7}$$

and

$$V_{01} = \sqrt{6}(-g_1)^{\frac{1}{3}}\bar{V}_{01}(\eta), \tag{3.8}$$

with the result that (3.6) becomes

$$\frac{\mathrm{d}^2\bar{V}_{01}}{\mathrm{d}\eta^2} - \eta\bar{V}_{01} = \bar{V}_{01}^3. \tag{3.9}$$

Note that $g_1(x)$, defined by (3.4*a*) is less than zero for all values of x. As noted by HL, (3.9) is a particular form of the second Painleve transcendent. It has been shown by Hastings & Mcleod (1978) that (3.9) has a solution such that

$$\bar{V}_{01} \sim (-\eta)^{\frac{1}{2}}, \quad \eta \to -\infty, \tag{3.10a}$$

and

$$\bar{V}_{01} \sim \sqrt{2}\,\mathrm{Ai}(\eta), \quad \eta \to +\infty. \tag{3.10b}$$

A solution for $\bar{V}_{01}$ was obtained numerically by using (3.10) and starting integrating at $\eta = +\infty$ in the direction of decreasing η using a fourth-order Runge–Kutta scheme. These results are used in the following analysis.

The results of Davey, DiPrima & Stuart (1968) show that the Taylor vortex flow is unstable against perturbations differing in phase from the fundamental component

of the steady vortex flow by $\frac{1}{2}\pi$. After instability, the new flow has wavy surfaces travelling in the azimuth separating neighbouring vortices. This suggests that, since we are seeking a secondary instability that will produce locally wavy vortex boundaries in IIa, b, we must consider a time-dependent perturbation to the basic flow in IIa, b which is $\frac{1}{2}\pi$ radians out-of-phase in the spanwise direction with the basic flow in IIa, b.

We have also considered the case of an in-phase perturbation and found the resulting problem more complicated than the present one. We anticipate that there are no unstable solutions for this case and just proceed with the present situation.

Hence, we seek solutions with out-of-phase perturbations proportional to

$$E = \exp\left(\frac{\mathrm{i}}{\epsilon^2}\int^x K(x)\,\mathrm{d}x - \frac{\mathrm{i}\Omega t}{\epsilon^2}\right). \tag{3.11}$$

Here the wavenumber K expands as

$$K = K_0 + \epsilon^{\frac{2}{3}}K_1 + \ldots, \tag{3.12}$$

and Ω is the constant frequency. It has of course been assumed that the wavy vortex mode is a short-wavelength high-frequency mode. This is necessary in order that this mode of secondary instability is trapped in the shear layers. We see later that this assumption is consistent with experimental observations. The lengthscale and timescale in (3.11) are chosen, from Hall (1982a), so that $\partial^2/\partial z^2 \sim \partial/\partial x$ and $\partial/\partial t + u\,\partial/\partial x = 0$ in the shear layer. The latter scaling ensures that the waves travel downstream with the speed of the fluid in the shear layer.

We find that the appropriate expansions in IIa take the form

$$u = u_{\mathrm{B}} + \left\{\delta\left(\epsilon^{\frac{4}{3}}\sin\left(\frac{z}{\epsilon}\right)E(u_{01} + \epsilon^{\frac{2}{3}}u_{11} + \ldots) + \ldots\right) + \ldots + \text{c.c.}\right\}, \tag{3.13a}$$

$$v = v_{\mathrm{B}} + \left\{\delta\left(\epsilon^{-\frac{2}{3}}\sin\left(\frac{z}{\epsilon}\right)E(v_{01} + \epsilon^{\frac{2}{3}}v_{11} + \ldots) + \ldots\right) + \ldots + \text{c.c.}\right\}, \tag{3.13b}$$

$$w = w_{\mathrm{B}} + \left\{\delta\left(\epsilon^{-\frac{1}{3}}\cos\left(\frac{z}{\epsilon}\right)E(w_{01} + \epsilon^{\frac{2}{3}}w_{11} + \ldots) + \epsilon^{-\frac{1}{3}}E(w_{m0} + \epsilon^{\frac{2}{3}}w_{m1} + \ldots) + \ldots\right) + \ldots + \text{c.c.}\right\}, \tag{3.13c}$$

$$p = p_{\mathrm{B}} + \left\{\delta\left(\epsilon^{-\frac{4}{3}}\sin\left(\frac{z}{\epsilon}\right)E(p_{01} + \epsilon^{\frac{2}{3}}p_{11} + \ldots) + \ldots\right) + \ldots + \text{c.c.}\right\}, \tag{3.13d}$$

where δ is a small amplitude and c.c. denotes complex conjugate. Note that there are only mean flow (independent of z) correction terms occurring in the expansion for w. This is a result of the perturbation being $\frac{1}{2}\pi$ radians out of phase with the fundamental vortex. For the case of an in-phase perturbation, mean flow correction terms also occur in the corresponding expansions for u, v, and p and the resulting eigenvalue problem is more complex.

The coefficients are functions of x and ξ and are determined by substitution of the expansions (3.13) into the unsteady equations of motion (2.4). The zeroth-order equations, obtained from equating coefficients of $\delta\sin(z/\epsilon)E$ in (2.4a–c) and $\delta\cos(z/\epsilon)E$ in (2.4d), are

$$\frac{\partial v_{01}}{\partial \xi} - w_{01} = 0, \tag{3.14a}$$

$$-\mathrm{i}\Omega u_{01} + \mathrm{i}K_0\,\bar{\bar{u}}_0\,u_{01} + v_{01}\frac{\partial \bar{\bar{u}}_1}{\partial \xi} = -u_{01}, \tag{3.14b}$$

$$-\mathrm{i}\Omega v_{01}+\mathrm{i}K_0\bar{\bar{u}}_0 v_{01}=-G_0\chi\bar{\bar{u}}_0 u_{01}-v_{01}, \tag{3.14c}$$

$$0=-p_{01}-w_{01}. \tag{3.14d}$$

Consistency of (3.14*b*, *c*) requires that

$$\Omega=K_0\bar{\bar{u}}_0. \tag{3.15}$$

This shows that the waves move downstream with mean speed $\bar{\bar{u}}_0$, i.e. the speed of the mean part of the basic flow in II*a*. Thus (3.14) reduces to

$$\frac{\partial v_{01}}{\partial\xi}-w_{01}=0, \quad u_{01}+\frac{\partial\bar{\bar{u}}_1}{\partial\xi}v_{01}=0, \quad w_{01}+p_{01}=0. \tag{3.16a–c}$$

Thus, once v_{01}, is obtained, equations (3.16) determine w_{01}, u_{01}, and p_{01}. (Note from (3.2) that $G_0\chi\bar{\bar{u}}_0\partial u_1/\partial\xi=1$). From equating coefficients of $\delta\sin z/\epsilon E$ in (2.4*b*, *c*) at the next order we obtain the equations

$$\mathrm{i}K_0\bar{\bar{u}}_1 u_{01}+\mathrm{i}K_1\bar{\bar{u}}_0 u_{01}+\frac{\partial\bar{\bar{u}}_1}{\partial\xi}v_{11}+\frac{\partial\bar{\bar{u}}_2}{\partial\xi}v_{01}-w_{m0}U_{01}=\frac{\partial u_{01}}{\partial\xi^2}-u_{11}, \tag{3.17a}$$

$$\mathrm{i}K_0\bar{\bar{u}}_1 v_{01}+\mathrm{i}K_1\bar{\bar{u}}_0 v_{01}-w_{m0}V_{01}=-G_0\chi\bar{\bar{u}}_0 u_{11}-G_0\chi\bar{\bar{u}}_1 u_{01}-\frac{\partial p_{01}}{\partial\xi}+\frac{\partial^2 v_{01}}{\partial\xi^2}-v_{11}. \tag{3.17b}$$

We substitute for v_{11} from (3.17*a*) into (3.17*b*) and use the solutions for $\bar{\bar{u}}_0$ and $\bar{\bar{u}}_1$ given by (3.2) to obtain

$$\frac{\partial^2 v_{01}}{\partial\xi^2}+g_1\xi v_{01}=\tfrac{1}{6}V_{01}^2 v_{01}-g_2 f v_{01}+\frac{2\mathrm{i}\Omega\xi v_{01}}{3(a+2y_2)}+\frac{2\mathrm{i}K_1(a+2y_2)^{\frac{1}{2}}v_{01}}{3(G_0\chi)^{\frac{1}{2}}}-\tfrac{2}{3}w_{m0}V_{01}. \tag{3.18}$$

Hence, in order to obtain a solution for v_{01} we require solutions for w_{m0} and the solution obtained from (3.3) for V_{01}. In order to determine w_{m0} we equate coefficients of δE in (2.4*d*). The resulting equation is

$$\mathrm{i}\Omega\frac{\bar{\bar{u}}_1}{\bar{\bar{u}}_0}w_{m0}+\mathrm{i}K_1\bar{\bar{u}}_0 w_{m0}+\tfrac{1}{2}V_{01}\frac{\partial^2 v_{01}}{\partial\xi^2}-\tfrac{1}{2}v_{01}\frac{\partial^2 V_{01}}{\partial\xi^2}=\frac{\partial^2 w_{m0}}{\partial\xi^2}. \tag{3.19}$$

On substitution of $\partial^2 v_{01}/\partial\xi^2$ and $\partial^2 V_{01}/\partial\xi^2$ from (3.18) and (3.3) respectively into (3.19) we obtain

$$\frac{\partial^2 w_{m0}}{\partial\xi^2}-\frac{\mathrm{i}\Omega\xi}{a+2y_2}w_{m0}-\frac{\mathrm{i}K_1(a+2y_2)^{\frac{1}{2}}}{(G_0\chi)^{\frac{1}{2}}}w_{m0}=-\tfrac{1}{3}w_{m0}V_{01}^2 + \frac{\mathrm{i}\Omega\xi}{3(a+2y_2)}v_{01}V_{01}+\frac{\mathrm{i}K_1(a+2y_2)^{\frac{1}{2}}}{3(G_0\chi)^{\frac{1}{2}}}v_{01}V_{01}. \tag{3.20}$$

Thus, it remains to solve the coupled equations (3.18) and (3.20) with the boundary conditions

$$v_{01}, w_{m0}\to 0 \quad \text{as } \xi\to\pm\infty. \tag{3.21}$$

If we look for a solution with K_1 of the form

$$K_1=\tilde{K}_1+\frac{\Omega g_2 f(G_0\chi)^{\frac{1}{2}}}{g_1(a+2y_2)^{\frac{3}{2}}}, \tag{3.22}$$

then, using the transformation (3.5), equations (3.18) and (3.20) become, respectively,

$$\frac{\partial^2 v_{01}}{\partial \xi_1^2} + g_1 \xi_1 v_{01} = \tfrac{1}{6} V_{01}^2 v_{01} + \frac{2i\Omega \xi_1 v_{01}}{3(a+2y_2)} + \frac{2i\tilde{K}_1 (a+2y_2)^{\frac{1}{2}} v_{01}}{3(G_0 \chi)^{\frac{1}{2}}} - \tfrac{2}{3} w_{m0} V_{01}, \tag{3.23}$$

and

$$\frac{\partial^2 w_{m0}}{\partial \xi_1^2} - \frac{i\Omega \xi_1 w_{m0}}{a+2y_2} - \frac{i\tilde{K}_1 (a+2y_2)^{\frac{1}{2}} w_{m0}}{(G_0 \chi)^{\frac{1}{2}}} = -\tfrac{1}{3} w_{m0} V_{01}^2 + \frac{i\Omega \xi_1 v_{01} V_{01}}{3(a+2y_2)} + \frac{i\tilde{K}_1 (a+2y_2)^{\frac{1}{2}} v_{01} V_{01}}{3(G_0 \chi)^{\frac{1}{2}}}. \tag{3.24}$$

For a fixed, real value of Ω we can solve (3.23) and (3.24) and determine the complex function $\tilde{K}_1(x)$ as x moves downstream. However, we are interested in neutrally stable solutions so we seek real values of Ω and $\tilde{K}_1(x)$. We can eliminate the x-dependence from the coefficients in (3.23) and (3.24) by making the transformations

$$v_{01} = (-g_1)^{-\frac{1}{3}} \bar{v}_{01}(\eta), \tag{3.25}$$

$$\tilde{K}_1 = \frac{\hat{K}_1 (G_0 \chi)^{\frac{1}{2}} (-g_1)^{\frac{2}{3}}}{(a+2y_2)^{\frac{1}{2}}}, \tag{3.26}$$

and

$$\Omega = \hat{\Omega}(-g_1)(a+2y_2). \tag{3.27}$$

Now we can find the constants $\hat{K}_1$ and $\hat{\Omega}$ so that the flow is neutrally stable at the location x where $\tilde{K}_1$ and Ω satisfy (3.26) and (3.27). Hence, with the transformations (3.7), (3.25), (3.26) and (3.27), equations (3.23) and (3.24) become, respectively,

$$\frac{d^2 \bar{v}_{01}}{d\eta^2} - (1 + \tfrac{2}{3} i\hat{\Omega}) \eta \bar{v}_{01} - \tfrac{2}{3} \hat{K}_1 \bar{v}_{01} = \bar{V}_{01}^2 \bar{v}_{01} - \tfrac{2}{3} \sqrt{6}\, w_{m0} \bar{V}_{01}, \tag{3.28a}$$

$$\frac{d^2 w_{m0}}{d\eta^2} - i\hat{\Omega} \eta w_{m0} - i\hat{K}_1 w_{m0} = -2 w_{m0} \bar{V}_0^2 + \tfrac{1}{3} \sqrt{6}\, i\hat{\Omega} \eta \bar{V}_{01} \bar{v}_{01} + \tfrac{1}{3} \sqrt{6}\, i\hat{K}_1 \bar{V}_{01} \bar{v}_{01}. \tag{3.28b}$$

We seek solutions of (3.28), with $\hat{K}_1$ and $\hat{\Omega}$ real, satisfying

$$v_{01}, w_{m0} \to 0 \quad \text{as } \eta \to \pm \infty. \tag{3.29}$$

As $\eta \to +\infty$ (3.28) can be written as

$$\frac{d^2 \bar{v}_{01}}{d\eta^2} - (1 + \tfrac{2}{3} i\hat{\Omega}) \eta \bar{v}_{01} - \tfrac{2}{3} i\hat{K}_1 \bar{v}_{01} = 0, \tag{3.30a}$$

and

$$\frac{d^2 w_{m0}}{d\eta^2} - i\hat{\Omega} \eta w_{m0} - i\hat{K}_1 w_{m0} = 0. \tag{3.30b}$$

Hence, as $\eta \to +\infty$ we can find two independent solutions for $\bar{v}_{01}$ and w_{m0}, in terms of the Airy function Ai, which satisfy (3.29). When $\eta \to -\infty$ the equations for $\bar{v}_{01}$ and w_{m0} are

$$\frac{d^2 \bar{v}_{01}}{d\eta^2} - \tfrac{2}{3} i\hat{\Omega} \eta \bar{v}_{01} - \tfrac{2}{3} i\hat{K}_1 \bar{v}_{01} = -\tfrac{2}{3} \sqrt{6}\, w_{m0} (-\eta)^{\frac{1}{2}}, \tag{3.31a}$$

$$\frac{d^2 w_{m0}}{d\eta^2} - (i\hat{\Omega} + 2) \eta w_{m0} - i\hat{K}_1 w_{m0} = \tfrac{1}{3} \sqrt{6}\, i\hat{\Omega} \eta (-\eta)^{\frac{1}{2}} \bar{v}_{01} + \tfrac{1}{3} \sqrt{6}\, i\hat{K}_1 \bar{v}_{01} (-\eta)^{\frac{1}{2}}. \tag{3.31b}$$

The appropriate expansions of (3.31) now take the form

$$\bar{v}_{01} = \exp[-\phi |\eta|^{\frac{3}{2}}] [\bar{v}_{010} + \ldots],$$

$$w_{m0} = |\eta|^{\frac{1}{2}} \exp[-\phi |\eta|^{\frac{3}{2}}] [w_{m00} + \ldots].$$

Here ϕ satisfies $$243\phi^4 + 36\phi^2(6+5i\hat{\Omega}) - 32\hat{\Omega}^2 = 0,$$

and we take the two roots of this equation with positive real part to generate two independent solutions of (3.31) with $\bar{v}_{01}, w_{m0} \to 0, \eta \to -\infty$.

These asymptotic solutions for $\bar{v}_{01}$ and w_{m0} at $\eta = \pm\infty$ were used as initial values in the numerical integration scheme used to solve (3.28). Equations (3.28) were written as a system of four first-order differential equations. This system was solved using a standard fourth-order Runge–Kutta integration scheme. The integration procedure was started at $\eta = -\infty$ and $\eta = +\infty$ and continued to $\eta = 0$, finding two independent solutions for $\bar{v}_{01}$ *and* w_{m0} from each direction. At $\eta = 0$ the continuity of a linear combination of the independent solutions from each direction produces an eigenvalue problem for $\hat{K}_1$ and $\hat{\Omega}$. We used a Newton–Raphson iteration scheme for two variables to find real values for $\hat{K}_1$ and $\hat{\Omega}$. Using the above scheme solutions for $\hat{K}, \hat{\Omega}, \bar{v}_{01}$ and w_{m0} were obtained but we postpone the discussion of these results until the next section.

Having found $\hat{\Omega}$ and $\hat{K}_1$ the dimensionless frequency and wavenumber, Ω and K respectively, can only be found once the HL calculation has been performed for a particular curvature distribution $\chi(x)$. However, HL gave asymptotic solutions of the free-boundary problem for x close to the linear neutral position, $x = x^*$, and for x a long way downstream of that position for curvature distributions which increase as quickly as $x^{\frac{1}{2}}$ for $x \gg 1$.

First, we recall that when $x \to x_+^*$ the shear layers coalesce. Thus if we denote by Ω_T and Ω_L the frequencies of the wavy vortex modes neutral in the upper and lower layers at x, it follows that

$$\frac{\Omega_L}{\Omega_T} \to 1, \quad x \to x_+^*. \tag{3.32}$$

Next suppose that $\chi \sim x^M, M > \frac{1}{2}$ for large x. Then the asymptotic forms for a, y_1, y_2 and b in this case are all given in HL. We find that g_{1T} and g_{1L}, the values of g_1, are given by

$$g_{1T} \sim \tfrac{1}{9}M x^{M-1} G_0, \quad g_{1L} \sim \frac{M^2}{27 G_0} x^{3M-2}. \tag{3.33}$$

(We note here in passing that g_1 in the lower layer is positive.) Thus for $x \gg 1$ we obtain

$$\Omega_T \sim \hat{\Omega}\tfrac{1}{9}M x^{2M-1} G_0^2, \quad \Omega_L \sim \tfrac{1}{3}\hat{\Omega},$$

or

$$\frac{\Omega_T}{\Omega_L} = \tfrac{1}{3}M G_0^2 x^{2M-1}.$$

It follows that as x increases, the frequency of the upper-layer mode which is neutral at x increases whilst that of the lower layer tends to a constant value. Thus we can distinguish between the modes as being of high and low frequency respectively; this result is entirely consistent with the experimental results discussed in the next section.

4. Results and discussion

The numerical scheme outlined above was used to search for eigenvalues $(\hat{K}_1, \hat{\Omega})$ in the region $\hat{K}_1 > 0, \hat{\Omega} > 0$. The only eigenvalues located were

$$(\hat{K}_1, \hat{\Omega}) = (4.156, 0.742). \tag{4.1}$$

It is possible that other eigenvalues exist at higher values of $\hat{K}_1, \hat{\Omega}$ since for

$|\hat{K}_1|, |\hat{\Omega}| > 0$ a detailed eigenvalue search was not carried out. When $\hat{\Omega}$ is zero the wavy modes are stable. Thus when $\hat{\Omega}$ is increased the mode described by (4.1) is more dangerous than any higher modes because it will occur first. However, at higher values of $\hat{\Omega}$ when all modes are unstable it is not clear which mode will have the biggest growth rate. Thus, we cannot say which will be the most dangerous mode. For any particular incoming boundary-layer profile the frequency Ω and wavenumber $K = K_0 + \epsilon^{\frac{4}{3}} K_1$ are then calculated from (3.12), (3.15), (3.22), (3.26), (3.27) and (4.1). This can only be done once the HL calculation has been carried out. The frequency and wavenumber obtained in this way will of course be dependent on x. The resulting expressions for Ω and K should be interpreted as the frequency and wavenumber that are neutrally stable at x. Alternatively, for a given frequency Ω, we could invert the equation

$$\Omega = \Omega(x, \epsilon),$$

to find the downstream location where the wavy vortex is neutrally stable. If Ω is held fixed at the neutral value at $x = \bar{x}$ then the wavenumber K becomes complex for $x \neq \bar{x}$. Then the wavy vortex mode undergoes spatial amplification or decay away from the neutral location.

We do not repeat the HL calculation in order to obtain specific values for K, Ω for a particular boundary-layer flow. We believe that the major result of this paper is that the large-amplitude states of HL are unstable in the thin shear layers that trap the vortices. The only available experimental results that give detailed results on the wavy mode structure do not give sufficient detail about the unperturbed boundary layer to enable us to calculate the relevant values of K and Ω. Hence, below we discuss only the qualitative agreement between our theory and these experimental results. However, before we compare our results with experiments, we shall first describe the eigenfunctions appropriate to (4.1).

These functions are shown in figures 2, 3 and we point out their oscillatory nature for negative values of η. We note that $\eta \to -\infty$ corresponds to moving from II$a, b$ into the core region I. It is of course possible that other 'lower-order' modes with a less oscillatory nature might exist but, as stated already, only those corresponding to (4.1) were found. In figure 4 we show the boundaries of the vortices in the shear layers II$a, b$ from above the region of vortex activity for the undisturbed flow and the wavy vortex modes.

Now let us turn to the physical implications and experimental relevance of our calculation. We first stress that the instability mechanism which we have described in detail for just the upper shear layer can also occur in the lower layer. If exponentially small terms are neglected, the modes of instability of the shear layers are independent because they decay exponentially away from the centre of the layers. However, the matching could in principle be carried out to show that an $O(1)$ disturbance in either layer would excite an exponentially small response in the other layer. Thus if we consider the frequency of the imposed wavy mode to be fixed, then the layers will break down in the manner described at different downstream locations. Since the downstream velocity component of the basic state is largest in the upper shear layer it is to be expected that this layer will be the first to become unstable. This follows from the zeroth-order eigenrelation (3.15) on the assumption that Ω is fixed and $\bar{\bar{u}}_0$ in IIa is bigger than $\bar{\bar{u}}_0$ in IIb. Furthermore, since the wavenumbers $K(x)$ appropriate to a fixed-frequency disturbances will be different, the modes propagate downstream with different wavespeeds. In fact initially, by which we mean close to the linear neutral position, the layers II$a, b$ coalesce. Thus, if breakdown occurs close to this point then the structure in these layers will be very

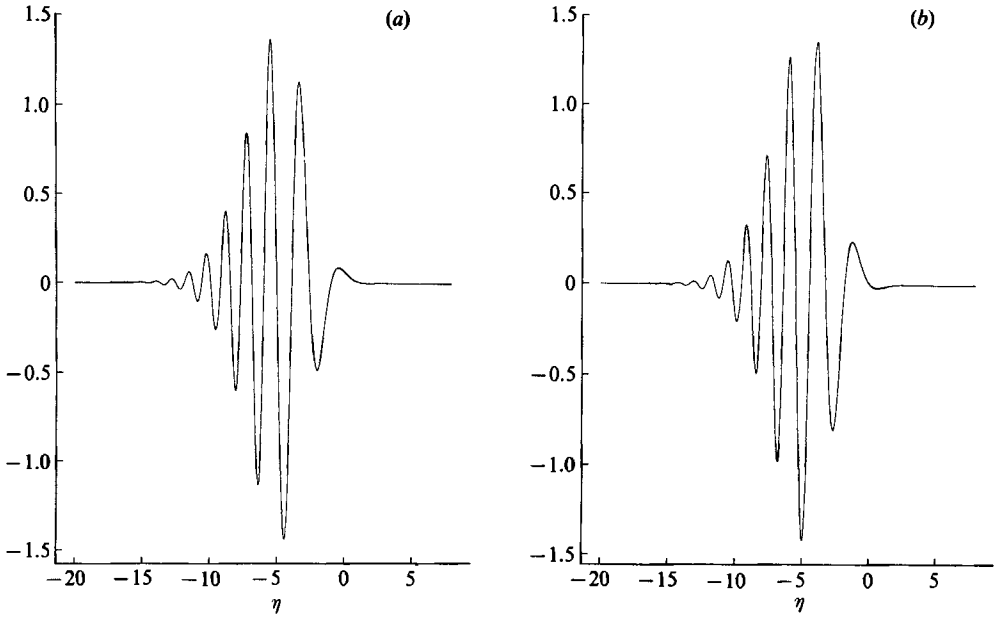

FIGURE 2. The neutral eigenfunction V_p for $(\hat{K}_1, \hat{\Omega}) = (4.156, 0.742)$ plotted against η: (*a*) Re (V_p), (*b*) Im (V_p).

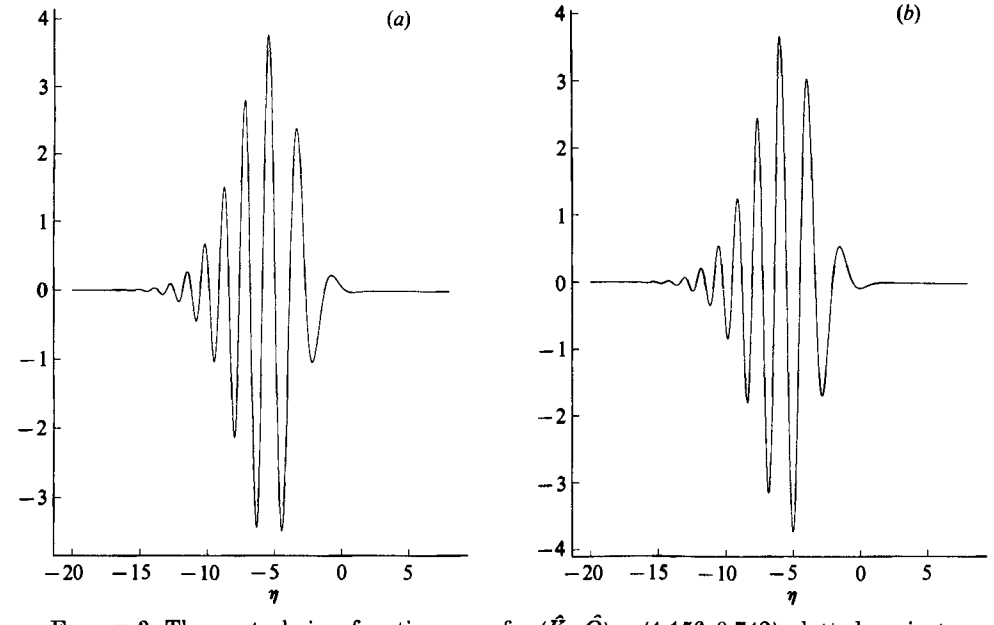

FIGURE 3. The neutral eigenfunctions w_{m0} for $(\hat{K}_1, \hat{\Omega}) = (4.156, 0.742)$ plotted against η: (*a*) Re (w_{m0}), (*b*) Im (w_{m0}).

similar. Further downstream the upper layer moves into the free stream and the downstream velocity component tends to the free-stream speed. The lower layer however approaches the boundary so that the fluid velocity there tends to zero. Thus, it follows that if the stationary Görtler vortices develop over a sufficiently long interval before breakdown then the upper-layer wavy mode moves downstream with

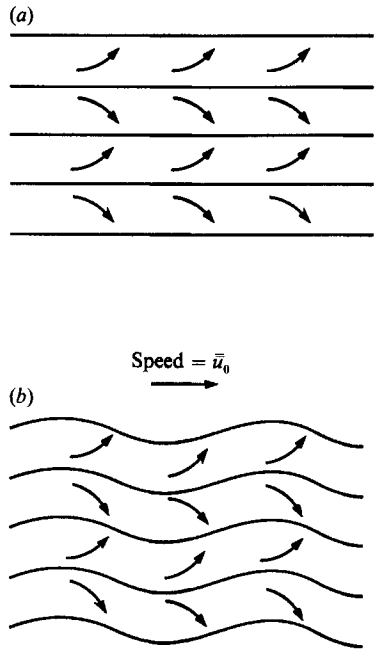

FIGURE 4. A section of the plan view of the boundaries separating neighbouring Görtler vortices in the shear layers IIa, b. The arrows show the direction of rotation of each vortex. (a) The fully developed undisturbed state. (b) The wavy vortex modes.

the free-stream speed whilst the lower one has a much smaller propagation speed. It is interesting to note that in the apparently closely related Taylor vortex problem the corresponding breakdown is due to a single wavy mode whose presence is felt throughout the flow.

There have been many experimental investigations of the secondary instability of Görtler vortices; the reader is referred to the papers by, for example, Bippes & Görtler (1972), Wortmann (1969), and Bippes (1978). These authors described the secondary mode as being locally periodic in x and t. However more recently Kohama (1987) and Peerhossaini & Wesfreid (1988) have given more details of the flow structure that exists when breakdown occurs. We first discuss the results of Peerhossaini & Wesfreid.

The boundary layer investigated by these authors was in the concave section of a curved channel. They found that when the secondary mode first appeared it was confined to a region at the top of the vortices. We interpret this as being due to the instability mechanism we have described being first operational in region IIa. Further downstream they reported a similar instability but this was localized near the wall. We interpret this instability as being due to the wavy vortex instability of region IIb. Both instabilities observed by Peerhossaini & Wesfreid had wavy vortex boundaries in the downstream direction, this is entirely consistent with the breakdown mechanism we have described in §3.

The experiments of Kohama were performed on the NASA laminar flow wing discussed by, for example, Pfenninger, Reed & Dagenhart (1980). Kohama described only the breakdown in the upper part of the boundary layer but gave measurements of the wavespeeds at different downstream locations. In the laminar flow region of the wing the wavespeed was found to be about 0.45 of the free-stream speed. This

factor became about 0.99 when the flow was fully turbulent. Such a variation of wavespeed is predicted qualitatively by our theory since the layer II*a* migrates from being somewhere in the middle of the boundary layer (more precisely at the position where Rayleigh's criterion for the pre-Görtler flow is most violated) to the edge as the vortices become fully nonlinear. The migration of this layer, we believe, accounts for the variation of wavespeed given by Kohama.

Finally we note that there are other instability mechanisms that could account for the appearance of three-dimensionality and time-dependence in the later stages of Görtler vortex development. The most likely other types of disturbances would be Rayleigh instabilities associated with the spanwise locally inflexional velocity profiles which certainly develop as the vortices develop in a steady manner. Secondly, there exists the possibility that Tollmien–Schlichting waves might cause the flow to become three-dimensional. However, it is not clear that these modes would lead to the wavy vortex boundaries which seem to be always observed when breakdown occurs. Nevertheless, it is likely that in some situations the Rayleigh and Tollmein–Schlichting modes might be important in the later stages of the transition process.

The authors would like to express their thanks to Dr A. P. Bassom for indicating an error in the original version of this work. The work was carried out while the second author was in receipt of an SERC research studentship. This research was supported under the National Aeronautics and Space Administration under NASA Contract No. NAS1-18107 while the authors were in residence at the Institute for Computer Applications in Science and Engineering (ICASE), NASA Langley Research Center, Hampton, VA 23665, USA.

REFERENCES

AIHARA, Y. & KOYAMA, H. 1981 Secondary instability of Görtler vortices: Formation of periodic three-dimensional coherent structures. *Trans. Japan Soc. Aero. Space Sci.* **24**, 78–94.

BIPPES, H. 1978 Experimental study of laminar turbulent transition of a concave wall in a parallel flow. *NASA TM* 75243.

BIPPES, H. & GÖRTLER, H. 1972 Dreidimensionales störungen in der grenzschicht an einer Konkaven Wand. *Acta. Mech.* **14**, 251–267.

DAVY, A., DIPRIMA, R. C. & STUART, J. T. 1968 On the instability of Taylor vortices. *J. Fluid Mech.* **31**, 17–52.

GÖRTLER, H. 1940 Uber eine dreidimensionale instabilität laminare Grenzschubten an Konkaven Wänden. *NACA TM* 1357.

HALL, P. 1982*a* Taylor–Görtler vortices in fully developed or boundary layer flows. *J. Fluid Mech.* **124**, 475–494.

HALL, P. 1982*b* On the nonlinear evolution of Görtler vortices in non-parallel boundary layers. *IMA J. Appl. Maths* **29**, 173–196.

HALL, P. 1983 The linear development of Görtler vortices in growing boundary layers. *J. Fluid Mech.* **130**, 41–58.

HALL, P. 1984 The Görtler vortex instability mechanism in three-dimensional boundary layers. *Proc. R. Soc. Lond.* A **399**, 135–152.

HALL, P. 1988 The nonlinear development of Görtler vortices in growing boundary layers. *J. Fluid Mech.* **193**, 247–266.

HALL, P. & LAKIN, W. 1988 The fully nonlinear development of Görtler vortices in growing boundary layers. *Proc. R. Soc. Lond.* A **415**, 421–444.

HASTINGS, S. P. & MCLEOD, J. B. 1978 A boundary value problem associated with the second Painleve transcendent. *Mathematical Research Center Rep.* 1861. University of Wisconsin.

HÄMMERLIN, G. 1956 Zür theorie der dreidimensionales instabilitat laminar Grenzschishten. *Z. Angew. Math. Phys.* **1**, 156–167.

KOHAMA, Y. 1987 Three-dimensional boundary layer transition on a convex-concave wall. In *Proc. Bangalore IUTAM Symp. on Turbulence Management and Relaminarisation* (ed. H. Liepmann & R. Narasimha). Springer.

PEERHOSSAINI, H. & WESFREID, J. E. 1988 On the inner structure of streamwise Görtler rolls. *Intl. J. Heat Fluid Flow* **9**, 12–18.

PFENNINGER, W., REED, H. L. & DAGENHART, J. R. 1980 Viscous flow drag reduction. *Prog. Astro. Aero.* **72**, 249–271.

SHAW, D. 1983 Stability and diffraction problems in incompressible fluid mechanics. Ph.D. Thesis, London University.

WORTMANN, F. X. 1969 Visualization of transition. *J. Fluid Mech.* **38**, 473–480.